Vol. 78: 225–236, 2019
https://doi.org/10.3354/cr01569

CLIMATE RESEARCH
Clim Res

Published online September 19

Tropical nights on the Spanish Mediterranean coast, 1950–2014

Jorge Olcina Cantos[1], Roberto Serrano-Notivoli[2], Javier Miró[3], Oliver Meseguer-Ruiz[4,*]

[1]Interuniversitary Institute of Geography, University of Alicante, Alicante 03690, Spain
[2]Estación Experimental de Aula Dei - Consejo Superior de Investigaciones Científicas (EEAD-CSIC), Zaragoza 50059, Spain
[3]Department of Earth Physics and Thermodynamics, University of Valencia, Valencia 46010, Spain
[4]Departamento de Ciencias Históricas y Geográficas, Universidad de Tarapacá, Arica 1010069, Chile

ABSTRACT: The increase in the number of tropical nights (TN; minimum temperature ≥ 20°C) constitutes important evidence of the global warming process throughout the Mediterranean region. A significant increase in the number of these events has been recorded since the second half of the 20th century. From the meteorological observations in the period 1950–2014 in the regions of Valencia and Murcia, in the central sector of the Spanish Mediterranean coast, we analyse the evolution of the number of tropical nights, the length of the episodes and their frequency. Our results indicate that the study regions experienced a significant increase in tropical nights within the last 3 decades due to climate change and the increase in sea surface temperatures (SST) in the central Western Mediterranean. We also discuss the relationship of the number of tropical nights with the increase in the Mediterranean Sea surface temperatures in the neighbouring sectors, as well as the possible implications of the combined effects of this with the urban heat island effect. Tropical nights are a cause of thermal discomfort, and thus there is a need to adapt buildings and manage urban planning to ameliorate this, and to be prepared for more frequent events in the future.

KEY WORDS: Tropical nights · Heat waves · Trends · Sea surface temperature · Spanish Mediterranean coast

1. INTRODUCTION

In the last few decades, temperatures have shown a clear and permanent change, leading to a warmer climate due to anthropogenic forcing (IPCC 2013) This is evidenced not only by mean temperatures, but also by episodes of extreme temperatures (Katz & Brown 1992). Extreme temperatures can have effects on a number of different aspects of the environment, including crop growth, distribution of agro-ecological regions, food supply and wildfires (Ye et al. 2013, Tian et al. 2017, Parente et al. 2018). In addition, temperatures above critical thresholds also cause a rise in morbimortality and human discomfort (Keellings & Waylen 2012, Gasparrini et al. 2015, Royé 2017). Tropical nights (TNs) occur when the minimum temperature is ≥ 20°C (Vincent et al. 2005, Alexander et al. 2006, WMO 2009, EEA 2012, Donat et al. 2013, Royé 2015), affecting human behaviour and rest. The Expert Team on Climate Change Detection and Indices used TNs as one of the climatic indicators to monitor climate change and analyse trends in the second half of the 20th century (Klein Tank et al. 2002). However, the concept of TNs has been employed in studies as early as the 1980s (Font Tullot 1983).

In the western Mediterranean context, TNs are linked with anticyclonic situations in western Europe in the mid-troposphere level. They most often occur in littoral areas and low plains, with Saharan air masses being an important source of hot air, helping to create extreme temperatures, even over periods of several days. From a climatic perspective, TNs on the

*Corresponding author: omeseguer@academicos.uta.cl

Spanish Mediterranean coast can be linked to: (1) heat wave episodes and (2) the high summer temperatures; both of these factors are relatively frequent in the Mediterranean region.

Heat waves have a substantial adverse impact on human health that can become more frequent under scenarios of increasing temperatures (Perkins-Kirkpatrick & Gibson 2017, Vicedo-Cabrera et al. 2018). Such events are especially harmful in areas affected by water scarcity, such as many areas in the Mediterranean basin, leading to negative effects on water resources and agriculture (Zittis et al. 2016). Several studies have shown that these kinds of events are increasing worldwide (Amengual et al. 2014, Piticar 2018, Wang et al. 2018) and will continue to increase (Barrera-Escoda et al. 2014). The occurrence of heat waves has been linked to sea surface temperature (SST) anomalies of both local and remote conditions (Purich et al. 2014), but studies have mainly focussed on oceanic scales (Ham & Na 2017, Deng et al. 2018). For instance, in the contiguous USA, the amplification of the Pacific zonal SST gradient has been associated with an increase in summer extreme heat waves (Deng et al. 2018). In addition, sea surface warming in the subtropical northwest Pacific causes heat waves in the Korean Peninsula with a delay of 7 d on average (Ha & Yun 2012, Min et al. 2015). In both cases, SST anomalies lead to changes in atmospheric circulation, which induce warmer and dryer conditions in the studied regions.

Apart from heat waves, TNs are strongly associated with summer temperatures, especially during the last decades. Different studies have shown a significant rise in the number of TNs in the eastern Mediterranean region (Zittis et al. 2016, Abbasnia & Toros 2018) as well as in the central (Boccolari & Malmusi 2013, Piccarreta et al. 2015, Scorzini et al. 2018) and western areas (Sanchez-Lorenzo et al. 2012, Barrera-Escoda et al. 2014, Royé & Martí Ezpeleta 2016). The summer temperature increase, which has been linked to the rise in Mediterranean water temperature (Pastor et al. 2018), has been particularly evident on the Spanish Mediterranean coast, with an increase in TNs over the last 3 decades (Basagaña et al. 2011, Royé 2017). This increase has important implications for impacts on socioeconomic activities, especially tourism, which generates ca. 10% of the gross domestic product of eastern peninsular Spain (Saurí et al. 2011). Recent changes in the climatic conditions, and those that may occur in the next few decades, will likely jeopardize the development of tourism; thus, adaptation measures for tourist destinations, both in urban planning and in building designs, will be needed (Olcina Cantos & Miró Pérez 2017). Potential effects on the tourist industry demonstrate the importance of studying this warming climatic phenomenon, as it generates thermal discomfort, and also leads to changes in other climate variables (e.g. precipitation) (Olcina Cantos 2017). Moreover, the increase in TNs and its relationship with the rising frequency of heat waves have direct implications on human health (Royé et al. 2018).

All of these negative impacts of TNs can be intensified by local effects and/or by future warming scenarios. Regarding local effects, the urban heat island (UHI) effect plays a key role. The characteristics of the urban environment, such as the extent of the urbanized surface, the shape of the urban grid and the types of buildings, create higher temperatures than rural environments, and night-time cooling is slower, generating higher discomfort in cities than in surrounding areas (Royé & Martí Ezpeleta 2015).

On the other hand, future climate projections outline an uncertain scenario where anomalous hot events (both TNs and heat waves) would become more frequent at the end of the century (Zittis et al. 2016) or even at a shorter temporal scale (Fallmann et al. 2017). In Spain, the patterns are very similar to the projected ones, with a known upward trend in TNs over the last decades (Sanchez-Lorenzo et al. 2011), and a future scenario with a more frequent occurrence of these episodes in 2050 (Barrera-Escoda et al. 2014).

The study of TNs is based on a fixed threshold (20°C), which might not be adequate for a comparison between all regions, due to the climatic differences between them. However, TNs have been demonstrated to be a good index for the Mediterranean region (Royé & Martí Ezpeleta 2015). Furthermore, the higher frequency of minimum temperatures exceeding 20°C in the last decades has led to the use of higher thresholds, promoting expressions such as 'equatorial nights' or 'torrid nights' (Pechs 2018) to emphasize the importance of these very warm nights. For example, Chen & Lu (2014) used a threshold of 25°C in their study of extreme warm nights in Beijing, and they differentiated 'TNa' (Tmin > 25°C) from 'pure TNs' considering the daily maximum temperature (Tmin > 25°C and Tmax < 35°C).

In this study, we present a comprehensive assessment of the spatial and temporal evolution of TNs in the central sector of the Spanish Mediterranean coast. In particular, we analyse the spatial distribution of the annual trends in (1) the frequency of TNs, (2) the maximum consecutive days of TN events and (3) the number of episodes with events >3 d (based on the usual definition of heat wave, we used 3 consecutive days to consider such TN heat waves [TNHWs]).

2. MATERIALS AND METHODS

2.1. Study area and temperature dataset

We used 668 series of daily minimum temperature data from within the territory of the Valencia and Murcia regions (34 568 km^2; Fig. 1b) at elevations ranging from 1 to 1720 m a.s.l. (study area ranges from 0 to 2027 m a.s.l.). The data covered the period 1950–2014 and were sourced from the Spanish Meteorological Agency (AEMET) (572 series) and the Spanish Ministry of Agriculture, Fisheries and Food (96 series).

The study area comprises one of the highest densities of meteorological observatories in Spain (approximately 1 station per 50 km^2 considering all the observations). Unfortunately, not all stations were recording during the whole period, which produces a high variability in the available information throughout the study period. The number of observations within the studied period increased from 90 recording stations in 1950 to more than 300 in 2014 (Fig. 1c).

With the aim of obtaining reliable and coherent spatial distributions and trends, we filled the gaps of all data series following an adaptation of the daily precipitation series-filling algorithm, fully described by Serrano-Notivoli et al. (2017). The method is based on the computation of temperature estimates in 3 steps: (1) calculating mean ± SD of monthly estimates through multivariate linear regressions (MLRs) based on all data and using latitude, longitude, altitude and distance to the coast as covariates, (2) refining these estimates for each month by computing them again with MLRs based only on the 15 nearest monthly observations plus the previously computed monthly value, with the same covariates and (3) calculating daily estimates through the same method but using the 15 nearest daily observations plus the refined monthly estimate. A final process of standardization applied to the daily estimates, using the refined mean and SD, provided the values used to fill the gaps.

All missing values in the original series were reconstructed, thus providing a complete dataset from which to analyse TN evolution. To assess the reliability of the reconstruction, the above method was not only applied to the missing data but also to those days with observations. This allowed a comparison

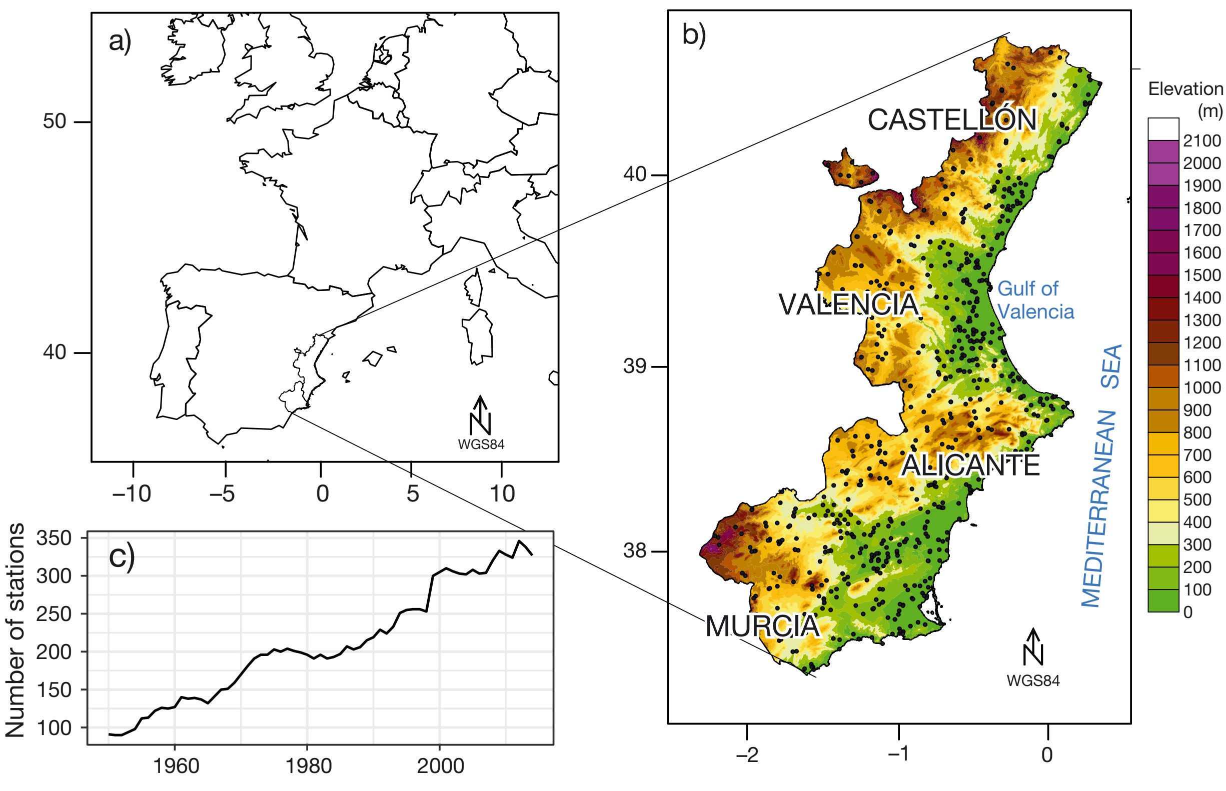

Fig. 1. (a,b) Study area (regions of Valencia and Murcia in Spain), elevation, regional division and location of all stations used in the study (black dots). Axes show decimal degrees. (c) Number of available recording stations over time

between the observations and their corresponding estimates by calculating the following set of statistics. We computed, by station, a goodness-of-fit (GOF) statistic: the mean absolute error (MAE), defined as the average of the absolute differences between observations and estimates; 2 bias statistics: the mean error (ME), which is the mean difference between observations and estimates and the ratio of means (RM), computed as the ratio between the mean of the observations and the mean of the estimates, and a comparison (Pearson correlation) of annual linear trends both in observations and reconstructed data. The results were aggregated by their median values, and their kernel density estimations (KDEs) were plotted. As the number of original observations was very different between stations, the statistics were calculated by dividing the dataset into 4 groups based on the number of original observations (all years, and more than 20, 30 and 40 yr) to avoid misinterpretations of the results.

2.2. TN analysis

In order to assess the spatial and temporal evolution of TNs in the study area, we first identified, at all stations, those days with minimum temperatures >20°C. We then grouped the resulting data series at 3 different (frequency, length and intensity) levels to obtain a set of 6 indices showing:

(1) the annual frequency (total sum of daily cases) of TN (TNF),

(2) the annual frequency of TN spells that encompass ≥ 3 d in length (TN3D),

(3) the annual mean first occurrence of TN (TNFirst),

(4) the annual mean last occurrence of TN (TNLast),

(5) the annual maximum length of TN hot spells (TNHS; consecutive TNs),

(6) the annual mean intensity of TNs (TNI; the difference between minimum temperature and the TN threshold of 20°C).

After this, a trend analysis was carried out to estimate the changes in these 3 indices through the application of nonparametric robust procedures for testing the existence of significant trends at all stations. These procedures were as follows:

(1) A Mann–Kendall trend test (Salmi et al. 2002) was applied for each of the available time series to assess the significance at $\alpha = 0.01$, $\alpha = 0.05$ and $\alpha = 0.1$ (Fig. 2). We considered different significance levels to evaluate if there is any influence in the spatial distribution of the station exhibiting the detected trends. Each station was classified according to whether it presented an upward (red point) or downward (blue point) significant trend. The achieved level of statistical confidence (or its absence) is displayed as a full coloured dot when confidence >99%, a semi-filled dot when confidence >95%, and a non-filled dot (only the circumference is coloured) when confidence >90%. When the trend is non-significant for any of the previous levels, a grey non-filled dot (grey circumference) is shown.

(2) The magnitudes of change were estimated using Sen's slope (Salmi et al. 2002). The annual slope values are presented in a spatially interpolated manner in the results, and must be analysed together with the Mann–Kendall test results to gauge the confidence of the slopes obtained over the analysed region.

In order to perform the spatial interpolation of Sen's slope results, a local polynomial interpolation technique was applied (Wang et al. 2018) as used by Miró et al. (2018). The interpolations were obtained as a denoised result with a spatial resolution of 400 m.

Since it is important to have a picture of the spatial distribution of TNF, TNHS and TNHW for a correct interpretation of changes in magnitude, a previous interpolation of their average annual values (1950–2014) was made (see Fig. 4) using the mentioned spatial interpolation technique.

3. RESULTS

3.1. Dataset validation

There were slight differences in goodness-of-fit (MAE) and bias (ME and RM) between the different datasets (Table 1). The MAE was near 1°C in all cases, while the ME was within a range of ±0.2°C. The RM was also near 1, indicating a very low bias between observations and estimates, but showing a progressive underestimation when reducing the number of stations. The comparison of trends showed a Pearson correlation near 0.9 when considering all stations and from 0.62 to 0.67 when the dataset was constrained to select a higher number of observations. Any estimation of the temporal series of an observed variable involves a reduction of the variance. These apparent large differences are likely due to (1) the low number of years in several series, causing very different trends with small changes in the estimates compared to the observations, and (2) the small values of annual trends that can be considered negligible (most of them are

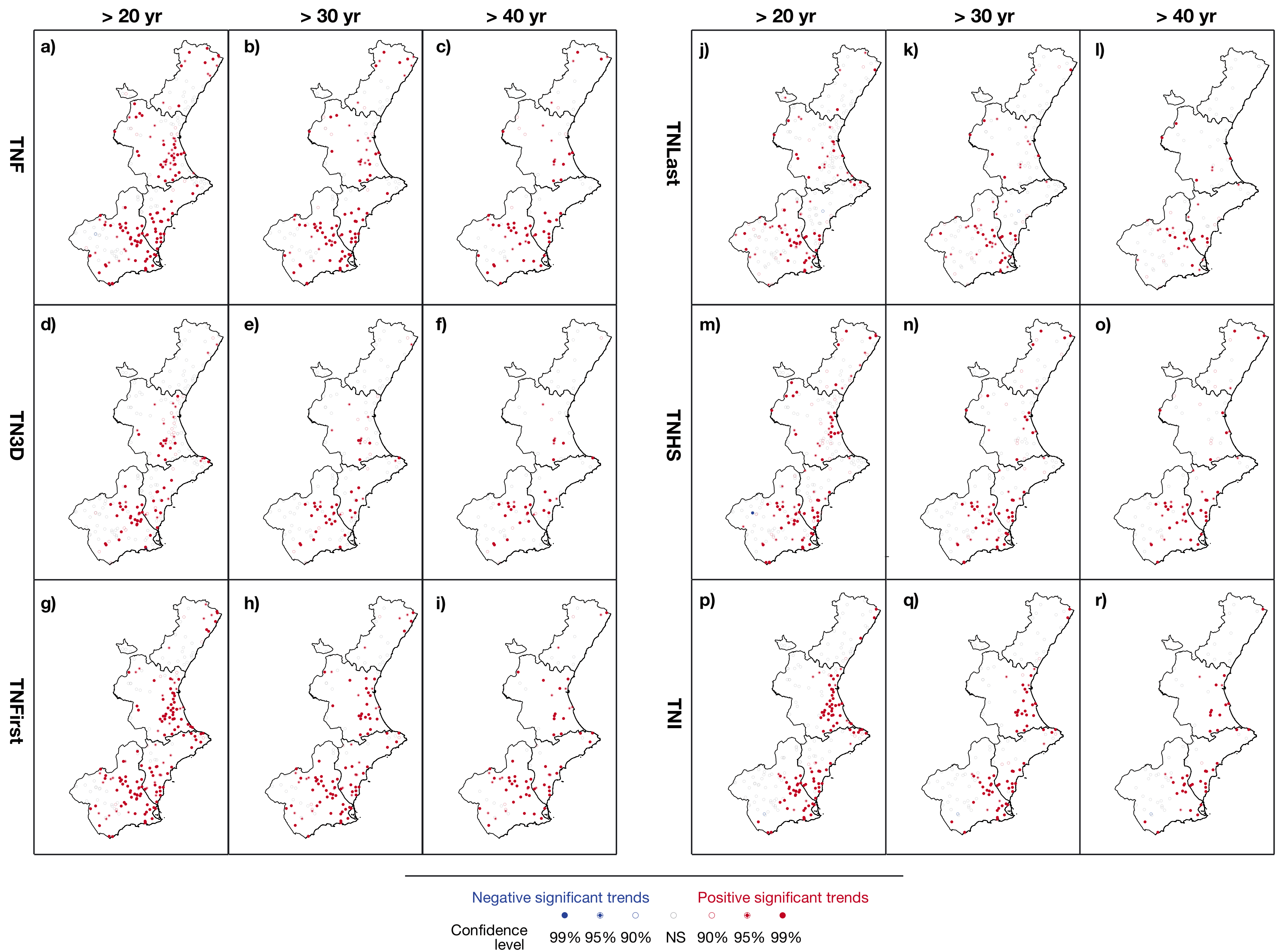

Fig. 2. Significance and sign of the trends, by station, using series with more than 20, 30 and 40 yr of original data for (a–c) the annual frequency (total sum of daily cases) of tropical nights (TNF), (d–f) the annual frequency of tropical night (TN) spells that encompass ‡ 3 d in length (TN3D), (g–i) the annual mean first occurrence of TN (TNFirst), (j–l) the annual mean last occurrence of TN (TNLast), (m–o) the annual maximum length of TN hot spells (TNHS) and (p–r) the annual mean intensity of TNs (TNI)

Table 1. Evaluation statistics (median values) comparing observations and their corresponding estimates for minimum temperature: mean absolute error (MAE) (°C), mean error (ME) (°C), ratio of means (RM) and Pearson correlation (all correlations are significant at 99%) of monthly linear trends (TC) considering all stations (All), and those with more than 20, 30 and 40 yr of original daily observations. **Bold:** best result for each statistic

Number of years	MAE	ME	RM	TC
All	**0.951**	0.121	1.011	**0.921**
>20	0.970	**0.002**	**1.000**	0.621
>30	1.022	−0.128	0.988	0.629
>40	1.037	−0.178	0.985	0.671

within the range of 1 SD, which is approximately ±0.1°C yr^{-1}). Since this error statistic can be misleading for the purposes of the research, we replicated the results in order to correctly evaluate the potential effect of reconstruction in trends. This replication consisted of mapping the trends of the indices using 3 separate datasets containing different numbers of stations from reconstructed series depending on the length of the original observations (more than 20, 30 or 40 yr). The comparison (Fig. 2) showed that a reduction in the number of stations did not change the spatial patterns of the significant trends in any of the 3 indices.

The KDE showed slight differences between datasets in the 3 error statistics (ME, MAE and RM), with lower influence of RM. The comparison of annual linear trends showed a good fit, being more dispersed when considering all stations due to the low number of years in some of the series, as mentioned above (Fig. 3).

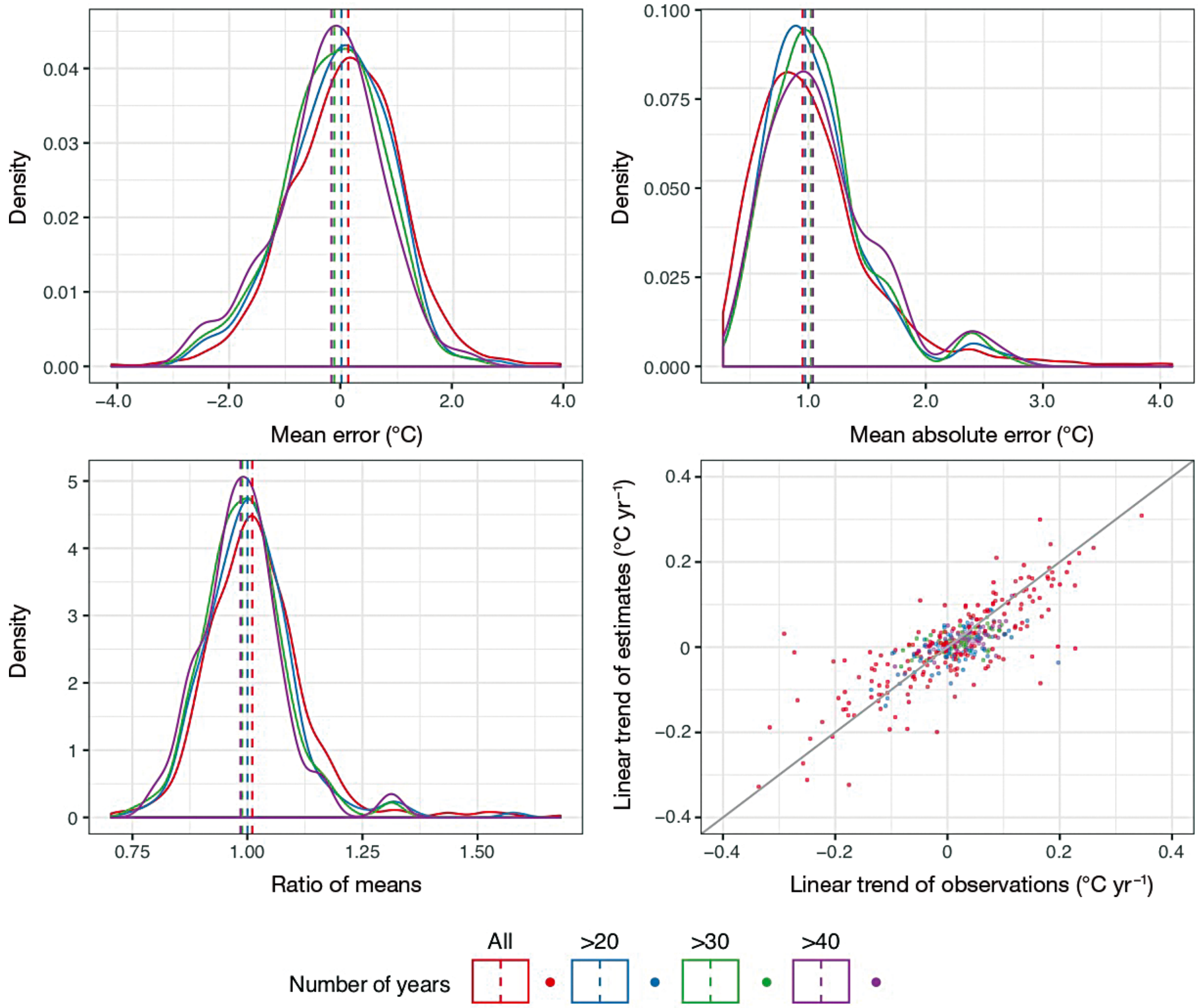

Fig. 3. Kernel density estimates of mean error (top left), mean absolute error (top right) and ratio of means (bottom left) considering different sets of data series based on the original number of years of recording data (coloured lines), and annual linear trend comparison (bottom right). Vertical dashed lines represent median values of the statistic

3.2. TN analysis

The 6 indices showed a similar spatial distribution, being aligned with the coastline in all cases. This may indicate spatial dependence with the SST of the Mediterranean Sea.

Regarding the frequency of TNs, the TNF (Fig. 4a) showed that the entire coastal strip normally registers >25 TNs yr^{-1}, a threshold that also extends into the pre-littoral fringe in the southern half of the region, with maximums exceeding 50 d on the coast of Alicante and Murcia, in contrast with most of the inland and high-elevation areas that usually register <5 d. When considering spells of ≥3 d, the TN3D index (Fig. 4b) showed a clearer latitudinal pattern with >5 events yr^{-1} on the coast of Murcia and Alicante (southern half), progressively decreasing to the north with 3 to 4 events along the northern half of the coastline. Again, a strong longitudinal gradient is revealed from higher values at the coast to a complete absence inland, especially emphasized in the northern half of the study area.

The indices describing the length of the TN season showed a clear longitudinal gradient highly influenced by the coastline. The TNFirst (Fig. 4c) showed earlier onset dates of the TN season on the coast (about mid-June) and a later one farther inland (around the end of July), coinciding with the highest elevations. An inverse pattern was found for the TNLast (Fig. 4d), with an average end of the TN season occurring in mid-September on the coast and in early August at high elevations. The annual maximum consecutive TNs (TNHS) (Fig. 4e) normally reached >20 d in the southern third of the region and 30 d in the southern extreme of Murcia. The rest of the study area was within the range of 10 to 20 d.

The intensity of the TN (TNI) (Fig. 4f) showed mean temperatures (>20°C) from 0.2 to 2°C. As with the other indices, a gradient from high values on the coastline to lower ones in inland areas was evident, indicating that the intensity of the TN is about 1 order of magnitude higher near the coast than in the rest of the study area.

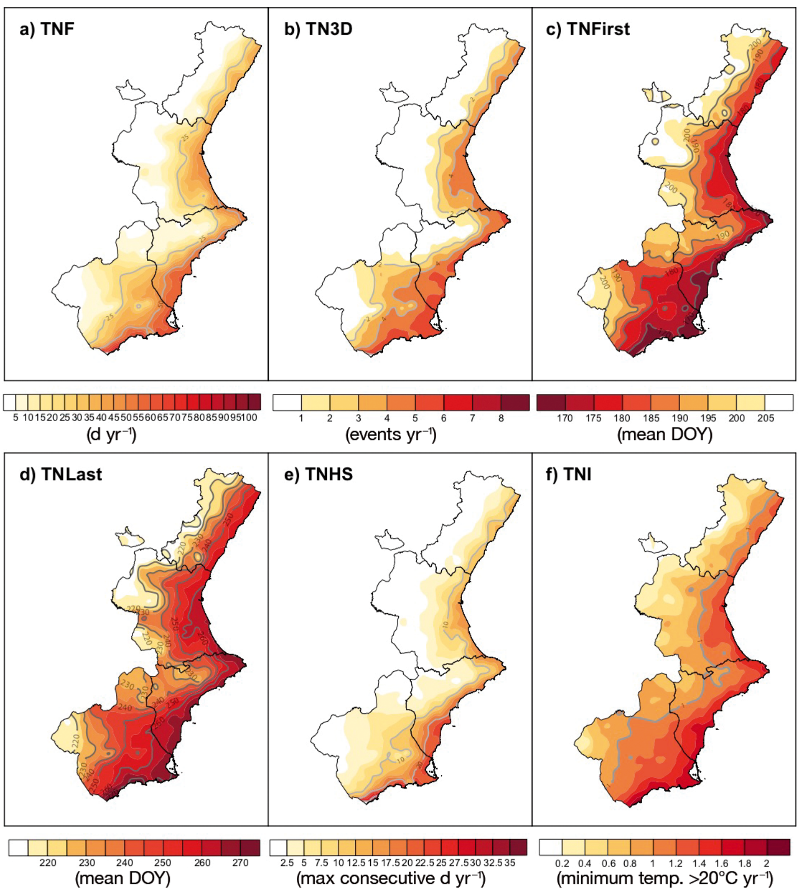

Fig. 4. Mean annual values (1950–2014) of tropical night (TN) frequency: (a) TNF, (b) TN3D; length: (c) TNFirst, (d) TNLast, (e) TNHS; and intensity: (f) TNI. DOY: day of the year; other abbreviations are defined in Fig. 2

The trend analysis for frequency indices showed a predominance of significant positive trends in TNF (Fig. 5a,c), especially in the littoral and pre-littoral southern and central areas of the study area. The zones in which no significant trends appeared coincided with inland and higher-elevation areas, where TNs are rare and their year to year occurrence is very irregular. The exception to this appears in the littoral sectors on the border between Castellón and Valencia, and on the border between Valencia and Alicante (non-significant weak changes). By contrast, the areas with the highest change and predominance of significant positive trends are the littoral and pre-littoral sectors close to the Gulf of Valencia and the south of Alicante together with the east and south of Murcia. These areas coincide with the main pre-littoral depressions, where annual slopes of change close to or above 0.5 d yr^{-1} are reached. This represents an increase of 32 d of absolute change between 1950 and 2014 in the annual frequency of TNs. Despite this, an average increase of 0.2 d yr^{-1} was reached for the whole study area (11 d of absolute change for

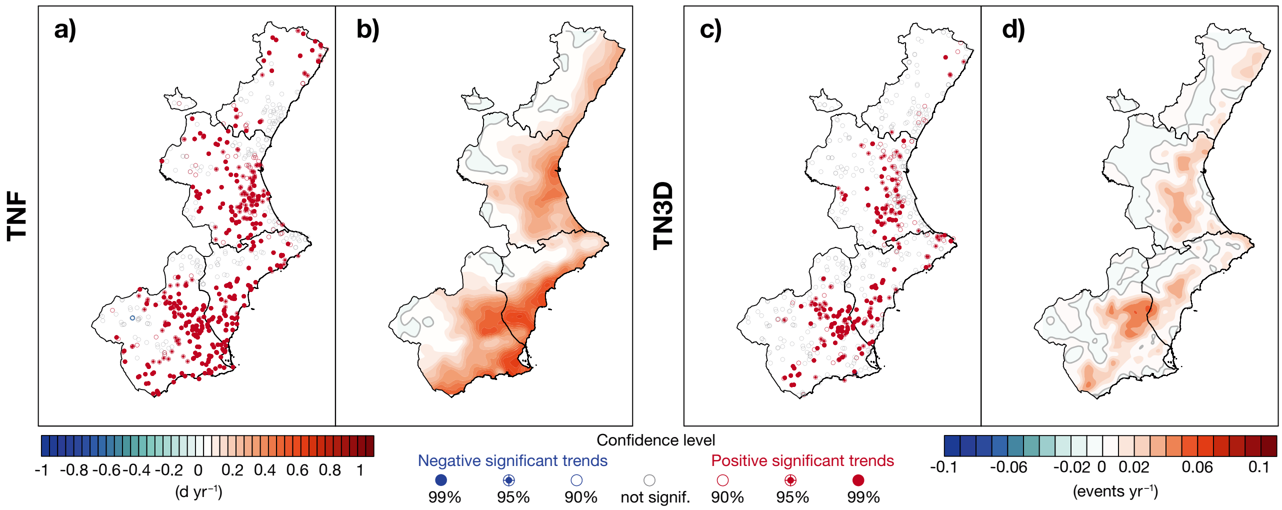

Fig. 5. Spatial distribution of tropical night frequency (TNF) trends (1950–2014) showing (a,c) the significance by station and (b,d) the interpolated rate of change of TNF and TN3D, respectively (abbreviations as in Fig. 2)

the entire period). However, an exception is shown for the case of the trends of TN3D (Fig. 5b,d). In this case, the main upward trends were not very common in the coastline areas in contrast to pre-littoral sectors, nearer to inland areas. These areas in Alicante and Murcia showed increases, in absolute numbers, between 2 and 3 events from 1950–2014 (0.03–0.05 occurrences yr^{-1}), as well as the northern part, which also showed an increase of around 2 events. The rest of the study area presented non-significant trends.

The spatial distribution of TN length trends showed general positive trends in TNFirst (Fig. 6a,b) and in TNLast (Fig. 6c,d), which means that the occurrence of TNs has been extended in both directions. Considering the studied period (1950–2014), TNs occur earlier, especially in the northern part, whereas the high inland elevations experienced a negative trend. On the other hand, the last TN of the year shows a belated occurrence, as this positive trend is more intense in mountainous areas than along the coastline. Regarding the TNHS (Fig. 6e,f), the increase was confined to a greater extent towards the coastal fringe. In particular, there was a strong increase on the coast of Murcia and Alicante (except at its north end) reaching ‡ 0.3 d yr^{-1}. Thus, the length of the maximum annual heat spell increased by 19 d between 1950 and 2014 in the southern area, and by 13 d (0.2 d yr^{-1}) on the central coast of the Gulf of Valencia. An increase of 0.1 d yr^{-1} was reached on the coast of Castellón. Although statistically significant positive trends appear elsewhere further inland from the coast, the increase is much weaker.

The trends of the intensity of the TNs (Fig. 7) showed a very low rate of change (within the range of ±0.2°C $decade^{-1}$), with higher values in coastal areas of Alicante and Valencia and negative values (near to 0) in inner areas of the northern part of the study area.

4. DISCUSSION

Based on a high-density station network, we analysed the occurrence of TNs in the central sector of the Spanish Mediterranean coast through several temperature-based indices representing the frequency, length and intensity of the phenomenon. Since the first time that TNs were mapped in Spain (Font Tullot 1983), showing a higher occurrence in the southern Iberian Peninsula, few other studies have addressed this topic (El Kenawy et al. 2011, Royé 2017). The results of our analysis are in line with this previous research and with others studying this variable in Mediterranean environmental trends (Sanchez-Lorenzo et al. 2011, Boccolari & Malmusi 2013, Piccarreta et al. 2015, Abbasnia & Toros 2018, Scorzini et al. 2018), exhibiting a clear positive trend in the second half of the 20th century. This generalized warming is consistent with the trends of most of the indices related to temperature, not only in our study area but also in the rest of the Mediterranean basin (Miró et al. 2006, Xoplaki et al. 2006, Hertig et al. 2010, Efthymiadis et al. 2011). Furthermore, the projected changes indicate that this trend will continue with different magnitudes depending on the considered climate change scenario (Barrera-Escoda et al. 2014, Zittis et al. 2016).

Our study shows that TN frequency and persistence have increased over time with a major influence

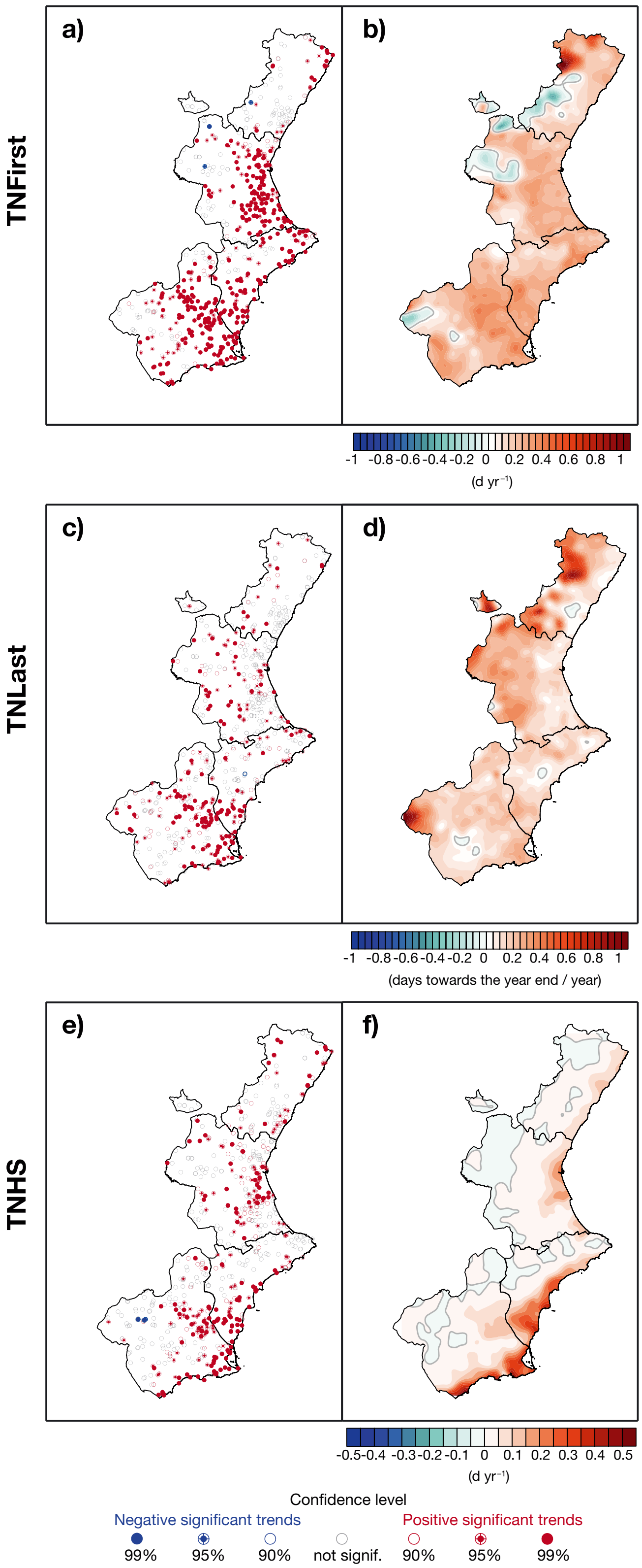

Fig. 6. Spatial distribution of TNFirst, TNLast and TNHS trends (1950–2014) showing (a,c,e) significance by station and (b,d,f) the interpolated rate of change of TNFirst, TNLast and TNHS, respectively (abbreviations as in Fig. 2)

of SST (discussed in Section 4.1), but the influence of SST is weak when considering the temporal evolution of events of long duration. TN frequency showed a clear association with the coastline, as did TN trends, which also exhibited an especially strong coastal pattern in the southern part of the study area. Moreover, while the TN hot spells and heat waves followed the same spatial distribution as the TN frequency, their corresponding increasing trends became diluted, where the initial trends were confined to a narrow line along the southern coast and the secondary trends were marginal and reduced to inland areas in the south.

The atmospheric mechanisms behind the increasing frequency of TNs are both large and synoptic in scale (Sanchez-Lorenzo et al. 2011). In the southwestern Pacific, the Asian Zonal Circulation and the Western Pacific Subtropical High drive these changes simultaneously (Wang et al. 2018). In the Western Mediterranean region, some circulation types transport air masses from the North Atlantic towards Europe, mostly in summer, when the Iberian thermal low appears, which is linked to a positive temperature anomaly (Santos et al. 2015, Michaelides et al. 2018).

4.1. SST influence

TN spatial and temporal behaviour in the studied area is directly linked with the Western Mediterranean SST, as noted by Purich et al. (2014). The littoral location of TNF, TNHS and TNHW confirmed this relationship, with no or very few events in inland locations, which can be also influenced by altitude in most inland regions. The mean temperature trends could be stronger on the mainland rather than in the coastal areas; however, minimum temperatures in higher-elevation inland regions are still usually below the 20°C threshold, as mentioned earlier.

Pastor et al. (2018) identified warming trends up to 2°C between 1982 and 2016 for summer months (mainly June and July), when TNs are more frequent. SST anomalies in summer present very different values and distributions from those recorded in winter. The relationship of such particular distributions and meteorological configurations leading to extreme events was identified by Pastor et al. (2018). Pastor et al. (2018) also reported that global warming has directly influenced SST warming rates during the present century. This may be accompanied with more frequent TNs in the future.

Pastor et al. (2018) also identified different spatial patterns in the SST warming trends for the Western

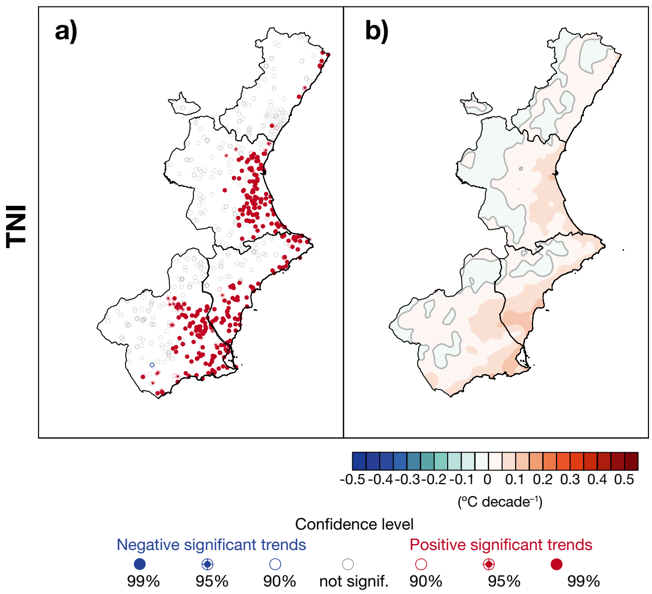

Fig. 7. Spatial distribution of tropical night intensity (TNI) trends (1950–2014) showing the significance by station (left) and the interpolated rate of change (right) of TNI

Mediterranean, being higher in the south of the studied area, close to the Alborán Sea. This could be related to the higher warming trends found in this study in the Murcia and Southern Valencia regions.

4.2. UHI influence

The sectors that show a greater increase in TNs match relatively well with areas that have experienced major urbanization processes and growing peri-urbanization of main urban centres (Valencia, Alicante and Murcia) throughout the period studied. This is a widely discussed problem in the scientific literature (e.g. Quereda-Sala et al. 2000, Royé & Martí Ezpeleta 2015) because it can distort the minimum temperatures and linked trends. Miró Pérez et al. (2015) performed statistical downscaling in the study region that reconstructed the temperature series observed from the low tropospheric reanalysis data. They concluded that, while a greater and generalized upward trend in maximum temperatures matched well with the downscaling, strong trends in the minimum temperatures in certain urban or peri-urban areas were not consistent with the downscaling. However, the results are consistent in rural areas and inland. This suggests that a predominance of surface-observed series affected by strong urbanization processes in the same area could confuse the correct signal in the homogenization process. Of course, the SST increase is also influential here; thus, it is very difficult to isolate the climate change signal from the urban effect with the current analysis (Barros Pozo & Martín-Vide 2018, Wiesner et al. 2018). However, even assuming there is some urban effect in certain areas, there is a clear underlying trend that TNs have increased throughout the region by 11 d on average for the whole region and the entire period 1950–2014. In addition, there was a generalized and greater (‡ 17 d) increase in the littoral fringe, which cannot be explained by the urban effect. In any case, the relationship between minimum temperatures and climate change is complex in mountainous regions. In the studied region, it has been estimated that the effects of climate change are clearer in the high parts of the mountains due to the upward trend in the frequency of nocturnal air temperature inversions (Miró Pérez et al. 2015, Miró et al. 2016).

5. CONCLUSIONS

The temporal evolution of frequency, length and intensity of TNs was analysed for the central sector of the Mediterranean coast of mainland Spain. The results showed a general increase in trends for the aforementioned 3 facets over the 1951–2014 period. The spatial distribution showed a strong influence of the coastline, indicating a potential effect of the Mediterranean Sea surface temperatures. This influence was also noted in the trends of the TN frequency and TNHS, but was less important in the trends of event duration.

Over the last few years, the scientific literature has highlighted the study of TNs in many areas of the world, including Spain. An increase in these overnight warm episodes has been proven along the Mediterranean coast, where the increase has been greater than in other areas.

This study has shown how the regions of Valencia and Murcia, in the central area along the Spanish Mediterranean coast, have experienced a significant increase in TNs within the last 3 decades. The causes are related to the global increase in temperatures due to the climate change process, but TNs have also acquired their own unique characteristics in this area due to the warming of SSTs in the central area of the Western Mediterranean basin (maritime sectors of Algiers and Gulf of Valencia).

The number of TNs has tripled in cities like Valencia or Alicante since 1980, which shows that we are experiencing an underlying trend where general and in factors converge. The increase of TNs in this Mediterranean region results in increasing nocturnal climatic discomfort, acting as a regional factor for a potential reduction in touristic competitiveness, not to mention the effects on tourism of other projected long-term climate changes to date (Greiving 2011, Ciscar et al. 2018).

These factors have forced policymakers to look for adaptive solutions that have tended to be short-term in nature and accompanied with high energy cost (e.g. air conditioning in housing and hotels). In the future, there will be a need to plan for urban layout that includes 'coolness islands' such as green areas and green infrastructure.

Acknowledgements. R.S.N. was funded by a 'Juan de la Cierva' postdoctoral grant FJCI-2017-31595. J.M. thanks the Spanish Ministerio de Economía y Competitividad and the European Regional Development Fund (FEDER) through the project CGL2015-64268-R (MINECO/FEDER, UE). O.M.R. thanks the Climatology Group (2017SGR1362, Catalan Government) and the CLICES Project (CGL2017-83866-C3-2-R).

LITERATURE CITED

Abbasnia M, Toros H (2018) Analysis of long-term changes in extreme climatic indices: a case study of the Mediterranean climate, Marmara Region, Turkey. Pure Appl Geophys 175:3861–3873

Alexander LV, Zhang X, Peterson TC, Caesar J and others (2006) Global observed changes in daily climate extremes of temperature and precipitation. J Geophys Res 111:D05109

Amengual A, Homar V, Romero R, Brooks HE, Ramis C, Gordaliza M, Alonso S (2014) Projections of heat waves with high impact on human health in Europe. Global Planet Change 119:71–84

Barrera-Escoda A, Gonçalves M, Guerreiro D, Cunillera J, Baldasano JM (2014) Projections of temperature and precipitation extremes in the North Western Mediterranean Basin by dynamical downscaling of climate scenarios at high resolution (1971–2050). Clim Change 122: 567–582

Barros Pozo PM, Martín-Vide J (2018) Influencia térmica antrópica local y global en el observatorio Fabra para el periodo 1924–2016. Bol Asoc Geogr Esp 79:1–19

Basagaña X, Sartini C, Barrera-Gómez J, Dadvand P and others (2011) Heat waves and cause-specific mortality at all ages. Epidemiology 22:765–772

Boccolari M, Malmusi S (2013) Changes in temperature and precipitation extremes observed in Modena, Italy. Atmos Res 122:16–31

Chen R, Lu R (2014) Large-scale circulation anomalies associated with 'tropical night' weather in Beijing, China. Int J Climatol 34:1980–1989

Ciscar JC, Feyen L, Ibarreta D, Soria A (coords) (2018) Climate impacts in Europe. Final report of the JRC PESETA III Project, European Commission. Publication Office of the European Union, Luxembourg

Deng K, Ting M, Yang S, Tan Y (2018) Increased frequency of summer extreme heat waves over Texas area tied to the amplification of Pacific Zonal SST gradient. J Clim 31: 5629–5647

Donat MG, Alexander LV, Yang H, Durre I and others (2013) Updated analyses of temperature and precipitation extreme indices since the beginning of the twentieth century: the HadEX2 dataset. J Geophys Res Atmos 118: 2098–2118

EEA (European Environment Agency) (2012) EEA Report: Urban adaptation to climate change in Europe: challenges and opportunities for cities together with supportive national and European policies, No. 2. European Environment Agency, Copenhagen

Efthymiadis D, Goodess CM, Jones PD (2011) Trends in Mediterranean gridded temperature extremes and large-scale circulation influences. Nat Hazards Earth Syst Sci 11: 2199–2214

El Kenawy A, López-Moreno JI, Vicente-Serrano S (2011) Recent trends in daily temperature extremes over northeastern Spain (1960-2006). Nat Haz Earth Syst Sci 11: 2583–2603

Fallmann J, Wagner S, Emeis S (2017) High resolution climate projections to assess the future vulnerability of European urban areas to climatological extreme events. Theor Appl Climatol 127:667–683

Font Tullot I (1983) Climatología de España y Portugal. INM, Madrid

Gasparrini A, Guo Y, Hashizume M, Lavigne E and others (2015) Mortality risk attributable to high and low ambient temperature: a multicountry observational study. Lancet 386:369–375

Greiving S (coord) (2011) ESPON CLIMATE — Climate change and territorial effects on regions and local economies. Final report. Technische Universität Dortmund, Dortmund

Ha KJ, Yun KS (2012) Climate change effects on tropical night days in Seoul, Korea. Theor Appl Climatol 109:191–203

Ham YG, Na HY (2017) Marginal sea surface temperature variation as a pre-cursor of heat waves over the Korean Peninsula. Asia-Pac J Atmospheric Sci 53:445–455

Hertig E, Seubert S, Jacobeit J (2010) Temperature extremes in the Mediterranean area: trends in the past and assessments for the future. Nat Hazards Earth Syst Sci 10: 2039–2050

IPCC (2013) Climate change 2013: the physical science basis. Contribution of Working Group I to the Fifth Assessment Report of the Intergovernmental Panel on Climate Change. Cambridge University Press, Cambridge

Katz RW, Brown BG (1992) Extreme events in a changing climate: variability is more important than averages. Clim Change 21:289–302

Keellings D, Waylen P (2012) The stochastic properties of high daily maximum temperatures applying crossing theory to modelling high-temperature event variables. Theor Appl Climatol 108:579–590

Klein Tank AMG, Wijngaard JB, Können GP, Böhm R and others (2002) Daily dataset of 20th century surface air temperature and precipitation series for the European Climate Assessment. Int J Climatol 22:1441–1453

Michaelides S, Karacostas T, Sánchez JL, Retalis A and others (2018) Reviews and perspectives of high impact atmospheric processes in the Mediterranean. Atmos Res 208:4–44

Min SK, Son SW, Seo KH, Kug JS and others (2015) Changes in weather and climate extremes over Korea and possible causes: a review. Asia-Pac J Atmospheric Sci 51:103–121

Miró JJ, Estrela MJ, Millán M (2006) Summer temperature trends in a Mediterranean area (Valencia region). Int J Climatol 26:1051–1073

Miró Peréz JJ, Estrela Navarro MJ, Olcina Cantos J (2015) Statistical downscaling and attribution of air temperature change patterns in the Valencia region (1948–2011). Atmos Res 156:189–212

Miró JJ, Estrela MJ, Caselles V, Olcina-Cantos J (2016) Fine-scale estimations of bioclimatic change in the Valencia region, Spain. Atmos Res 180:150–164

Miró JJ, Estrela MJ, Caselles V, Gómez I (2018) Spatial and temporal rainfall changes in the Júcar and Segura basins (1955–2016): finescale trends. Int J Climatol 2018: 4699–4722

Olcina Cantos J (2017) Incremento de episodios de inundación por lluvias de intensidad horaria en el sector central del litoral mediterráneo español: análisis de tendencias en Alicante. Semata 29:143–163

Olcina Cantos J, Miró Pérez JJ (2017) Actividad turística y cambio climático en la Comunidad Valenciana. Universidad de Alicante, Instituto Universitario de Investigaciones Turísticas, Agència Valenciana del Turisme, Valencia

Parente J, Pereira MG, Amraoui M, Fischer EM (2018) Heat waves in Portugal: current regime, changes in future climate and impacts on extreme wildfires. Sci Total Environ 631–632:534–549

Pastor F, Valiente JA, Palau JL (2018) Sea surface temperature in the Mediterranean: trends and spatial patterns (1982–2016). Pure Appl Geophys 175:4017–4029

Pechs JIC (2018) An extreme heat vulnerability assessment for the metropolitan area of Barcelona. A technical guide to calculate vulnerability and recommendations for future action and study. MSc thesis, University of Barcelona

Perkins-Kirkpatrick SE, Gibson PB (2017) Changes in regional heatwave characteristics as a function of increasing global temperature. Sci Rep 7:12256

Piccarreta M, Lazzari M, Pasini A (2015) Trends in daily temperature extremes over the Basilicata region (southern Italy) from 1951 to 2010 in a Mediterranean climatic context. Int J Climatol 35:1964–1975

Piticar A (2018) Changes in heat waves in Chile. Global Planet Change 169:234–246

Purich A, Cowan T, Cai W, van Rensch P and others (2014) Atmospheric and oceanic conditions associated with Southern Australian heat waves: a CMIP5 analysis. J Clim 27:7807–7829

Quereda-Sala J, Gil-Olcina A, Pérez-Cueva A, Olcina-Cantos J, Rico-Amorós A, Montón-Chiva E (2000) Climatic warming in the Spanish Mediterranean: natural trend or urban effect. Clim Change 46:473–483

Royé D (2015) Another approach for tropical nights: case studies of Faro, Lisbon and Porto. The overarching issues of the European space: spatial planning and multiple paths to sustainable and inclusive development. FLUP, Porto, p 269–283

Royé D (2017) The effects of hot nights on mortality in Barcelona, Spain. Int J Biometeorol 61:2127–2140

Royé D, Martí Ezpeleta A (2015) Análisis de las noches tropicales en la fachada atlántica de la Península Ibérica. Una propuesta metodológica. Bol Asoc Geogr Esp 69:351–368

Royé D, Martí Ezpeleta A (2016) Análisis espacio-temporal de las noches cálidas en el litoral mediterráneo de España. In: Olcina Cantos J, Rico Amorós A, Moltó Mantero E (eds) Clima, sociedad, riesgos y ordenación del territorio. Instituto Interuniversitario de Geografía, Universidad de Alicante: Asociación Española de Climatología, Alicante, p 689–700

Royé D, Figueiras A, Taracido M (2018) Short-term effects of heat and cold on respiratory drug use. A time-series epidemiological study in A Coruña, Spain. Pharmacoepidemiol Drug Saf 27:638–644

Salmi T, Määttä A, Anttila P, Ruoho-Airola T, Amnell T (2002) Detecting trends of annual values of atmospheric pollutants by the Mann–Kendall Test and Sen's slope estimates — the excel template application MAKESENS. Publication on Air Quality 31. Finnish Meteorological Institute, Helsinki

Sanchez-Lorenzo A, Pereira P, Lopez-Bustins JA, Lolis CJ (2012) Summer night-time temperature trends on the Iberian Peninsula and their connection with large-scale atmospheric circulation patterns. Int J Climatol 32: 1326–1335

Santos JA, Pfahl S, Pinto JG, Wernli H (2015) Mechanisms underlying temperature extremes in Iberia: a Lagrangian perspective. Tellus A Dyn Meteorol Oceanogr 67:26032

Saurí D, Olcina J, March H, Martín-Vide J, Vera F, Padilla E, Serra-Llobet A (2011) Case study Mediterranean coast of Spain. In: ESPON CLIMATE: Climate change and territorial effects on regions and local economies. Applied research project 2012/1/4. Final Report. Annex 4. www.espon.eu/climate (accessed 21 Oct 2018)

Scorzini AR, Di Bacco M, Leopardi M (2018) Recent trends in daily temperature extremes over the central Adriatic region of Italy in a Mediterranean climatic context. Int J Climatol 38:e741–e757

Serrano-Notivoli R, de Luis M, Saz MÁ, Beguería S (2017) Spatially based reconstruction of daily precipitation instrumental data series. Clim Res 73:167–186

Tian J, Liu J, Wang J, Li C, Nie H, Yu F (2017) Trend analysis of temperature and precipitation extremes in major grain producing area of China. Int J Climatol 37:672–687

Vicedo-Cabrera AM, Guo Y, Sera F, Huber V and others (2018) Temperature-related mortality impacts under and beyond Paris Agreement climate change scenarios. Clim Change 150:391–402

Vincent LA, Peterson TC, Barros VR, Marino MB and others (2005) Observed trends in indices of daily temperature extremes in South America 1960-2000. J Clim 18:5011–5023

Wang L, Wang WJ, Wu Z, Du H, Shen X, Ma S (2018) Spatial and temporal variations of summer hot days and heat waves and their relationships with large-scale atmospheric circulations across Northeast China. Int J Climatol 38:5633–5645

Wiesner S, Bechtel B, Fischereit J, Gruetzun V and others (2018) Is it possible to distinguish global and regional climate change from urban land cover induced signals? A mid-latitude city example. Urban Sci 2:12

WMO (2009) Analysis of extremes in a changing climate in support of informed decisions for adaptation. WCDMP-No. 72. World Meteorological Organization, Geneva

Xoplaki E, Luterbacher J, González-Rouco JF (2006) Mediterranean summer temperature and winter precipitation, large-scale dynamics, trends. Nuovo Cimento C 29:45–54

Ye L, Yang G, Van Ranst E, Tang H (2013) Time-series modelling and prediction of global monthly absolute temperature for environmental decision making. Adv Atmos Sci 30:382–396

Zittis G, Hadjinicolaou P, Fnais M, Lelieveld J (2016) Projected changes in heat wave characteristics in the eastern Mediterranean and the Middle East. Reg Environ Change 16:1863–1876

Editorial responsibility: Toshichika Izumi, Tsukuba, Japan

Submitted: March 11, 2019; Accepted: July 15, 2019
Proofs received from author(s): September 6, 2019